

An Analytical Investigation of the Flow in the Saturated Zone of Ice Counterwashers

AMITZUR BARAK

Israel Desalination Engineering, Tel Aviv, Israel

and GEDEON DAGAN

Israel Institute of Technology, Haifa, Israel

The flow of brine through the ice bed in gravitational counterwashers is investigated by analytical methods. Two types of counterwashers are considered: a drained-top counterwasher and a flooded one. Only counterwashers of rectangular cross section and two dimensional flows are investigated. By assuming that the ice crystals move vertically upwards with a uniform velocity and that the relative flow of brine and wash water with respect to the ice bed obeys Darcy's law, the differential equations and the boundary conditions of the flow are derived. The solutions are obtained by using complex variables and conformal mapping. The solutions are presented as formulae, which make possible the rational design of counterwashers and the optimization of their dimensions and operation parameters.

Ice counterwashers (noted subsequently as CW) are used in freeze desalination processes for separating ice crystals from brine.

The CW is a vertical column with vertical drainage screens (Figures 1 and 2) on its walls, in the middle zone.

The mixture of brine and ice particles, which is generated in the previous stage of the process, enters the bottom of the CW as a suspension, and the ice particles consolidate and form a compact porous bed above a certain level AG (Figure 1, 2).

The ice bed moves upwards due to buoyancy and the drag of the brine, which percolates through it to the screens BD. The movement of the ice bed is opposed by the friction at the walls, the resistance of the mechanical scraper, which harvests the ice at the top of the column and transfer it out of the CW (to be melted) and the weight and drag of the desalted wash water, by which the ice is washed from the remaining brine at the top of the column, just below the scraper.

Two types of CW are considered in this paper: (a) the drained-top counterwasher (DCW) and (b) the flooded one (FCW).

In the case of DCW (Figure 1) the brine saturates the porous ice bed up to a free surface EF. Above this surface the bed is unsaturated. Fresh wash water is sprayed on the top of the ice bed and seeps downward due to gravity through the unsaturated zone, washing the ice this way. Part of the fresh water flux reaches the free surface and flows towards the screen, where it drains out with the brine. In general this fresh water loss does not exceed a few percent of the ice production. The rest of the wash water adheres to the washed ice.

In the case of the FCW (Figure 2) the entire ice bed is saturated. The wash water is forced to flow through the ice bed under pressure.

Theoretical and experimental studies on CWs have been published by Barduhn (1), Bosworth, et al. (2, 3), Hahn (4, 5), Kuivenhoven (6), Mixon (7), Sherwood and Brian (8), Wiegandt (9) and others. One of the conclusions expressed in these reports is that most of the washing process, that is, the removal of the dissolved salts from the ice by the wash water, takes place only in a small portion of the upper zone of the column. The dimensions of the CW depend on the flow pattern in it rather than on the washing process.

The aim of the present work is to solve the problem of the flow through the ice bed in its saturated part. More

specifically, to find the fields of the hydrostatic pressure (p), the local superficial velocity (\tilde{q}), and the stream function (ψ), as the functions of the various parameters of the wash columns.

The solution enables a rational design of any desired CW, optimization of its parameters and quantitative control of its performance.

In the present analysis the concepts of drainage theory are used in order to solve the problem.

BASIC ASSUMPTIONS

The present analysis is based on the following assumptions:

1. The flow is two dimensional, that is, the CW is of rectangular cross section and the screens are installed symmetrically on two opposite walls.
2. The flow relative to the porous medium obeys Darcy's law. A detailed analysis (10) shows that for ice particles with equivalent hydraulic diameter less than $\frac{1}{2}$ mm. the validity of Darcy's law is ensured.
3. The screens are submerged in brine, otherwise the wash water may freeze and clog the upper part of the screens, the temperature of which is sometimes lower than 32°F ., probably due to heat conduction to the lower part which is in contact with brine at approximately 26°F .
4. Both vertical distances from the center of the screens to the bottom of the ice bed (d) and to the upper boundary of the saturated zone (h) are at least equal to $b + a$, where $2b$ is the width of the CW and $2a$ the height of the screens. This restriction, which is generally met in typical installations, simplifies the mathematical analysis considerably.
5. The porous bed is homogeneous, isotropic, and non-deformable; the porosity (n), the permeability (k), and the ice velocity (U), upward are uniform.
6. The density (ρ), the viscosity (μ) of the liquid phase in the saturated zone and therefore the hydraulic conductivity (K) are practically uniform; the small variations due to the salinity gradient are negligible.
7. There is no mass transfer between the phases.
8. The flow is steady.

The present work is based on the report (10). In the interval between the publication of this report and that of the present paper, the problem of flow in CWs has been treated by two other teams. A similar analytical approach has been used by Schwartz and Probstein (11). An elec-

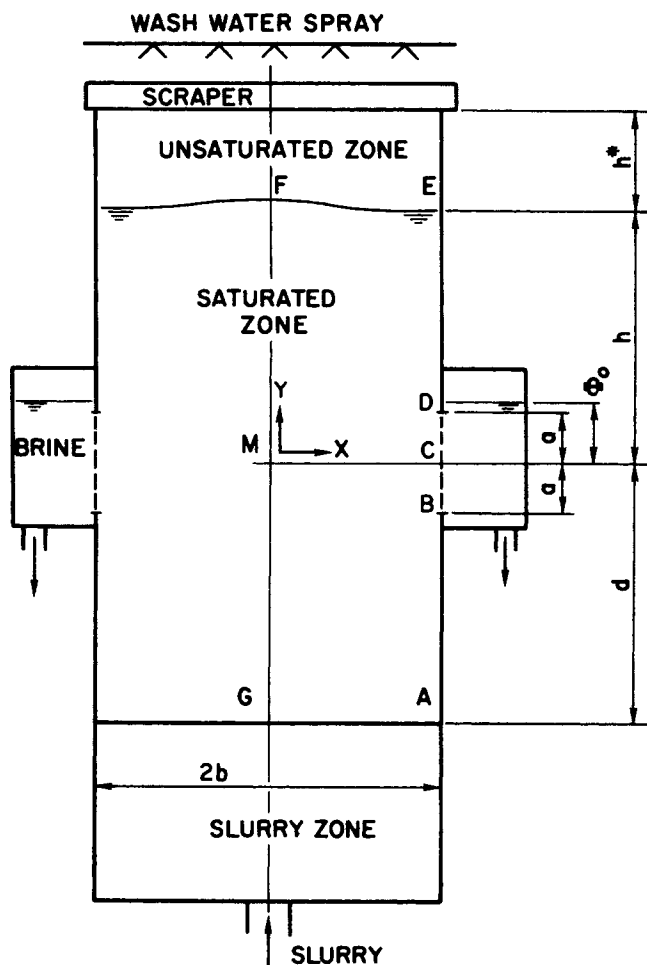


Fig. 1. Schematic diagram of a drained-top counterwasher.

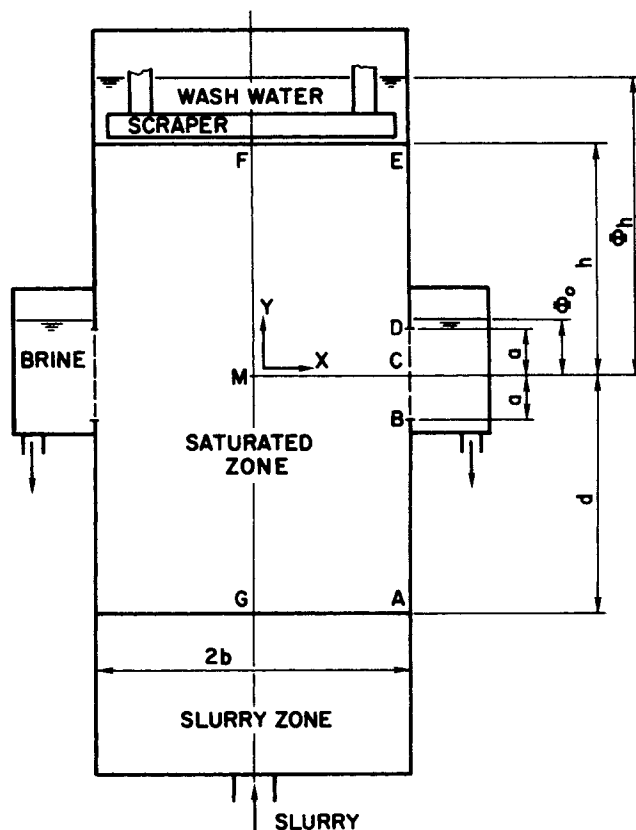


Fig. 2. Schematic diagram of a flooded counterwasher.

(K), and the specific weight (γ) of the liquid are defined by

$$\phi = \frac{p}{\gamma} + y; \quad K = \frac{k\gamma}{\mu}; \quad \gamma = \rho g \quad (2)$$

y is the height above an arbitrary reference level (in our case, the horizontal center line of the screens).

Equation (1) differs from the Darcy's law by the term $n \tilde{U}$ at the right hand side.

The continuity law gives:

$$\text{div } \tilde{q} = 0 \quad (3)$$

Hence, we get from (1) and (3) the Laplace equation for ϕ :

$$\text{div grad } \phi = \nabla^2 \phi = 0 \quad (4)$$

because n , K , and U were assumed constant.

In the case of two dimensional flow it is convenient to use, in addition to the head, the stream function (ψ) and the potential (φ) of the absolute liquid superficial velocity (\tilde{q}). By definition

$$q_x = -\frac{\partial \varphi}{\partial x} = -\frac{\partial \psi}{\partial y}; \quad q_y = -\frac{\partial \varphi}{\partial y} = \frac{\partial \psi}{\partial x} \quad (5)$$

It is easy to ascertain that the following relationships hold as a consequence of the previous equations:

$$\nabla^2 \varphi = 0; \quad \nabla^2 \psi = 0 \quad (6)$$

$$\varphi(x, y) = K \phi(x, y) - nUy + \varphi_0 \quad (7)$$

x is the horizontal distance from an arbitrary vertical line, in our case the centerline of the CW. φ_0 is an arbitrary constant.

The functions φ and ψ are, according to Equations (5)

trical analog (Teledeltos resistance paper) has been used by Wiegandt, Von Berg, and Leinroth (12). In both works, however, only the case of FCW is treated while in the present paper both FCW and DCW, which is more practical at present, are studied. Moreover, Schwartz and Probstein assume that the screens may be represented by a sink-point or several sink-points rather than a line of constant head, as assumed here. This additional approximation restricts the application of the results to CW having relatively short screens. They also disregard, in their analysis, the possibility of brine breakthrough to the wash water.

Wiegandt, Von Berg, and Leinroth (12) provide eighteen solutions of particular cases of different configurations. A complete solution of the general case cannot be obtained due to the nature of the analog method. The high number of independent variables requires a system of many specific solved cases for each configuration to enable the correlation of these variables and the other dependent parameters. On the other hand the versatility of this analog method enables an interesting comparison of CWs of different configurations and this comparison is accomplished by Wiegandt, et al. (12).

MATHEMATICAL REPRESENTATION OF THE PROBLEM

The differential equation of the piezometric head (ϕ) is obtained from the Darcy-Gerzevanov's law (13):

$$\tilde{q} = n \tilde{U} - K \text{ grad } \phi \quad (1)$$

where the piezometric head, the hydraulic conductivity

harmonic conjugate functions, satisfying the Cauchy-Riemann equations; that is, they are the real and imaginary part, respectively, of an analytical complex potential

$$\omega(z) = \varphi(x,y) + i\psi(x,y) \quad (8)$$

where

$$z = x + iy \quad (9)$$

The theory of complex variables will be used subsequently in order to solve the flow problem.

BOUNDARY CONDITIONS

The boundaries of DCW are given in Figure 3. AB, DE, and FG are vertical streamlines (AB and ED being impervious walls and FG being a symmetry line), for which

$$\frac{\partial \psi}{\partial y} = 0; \quad \frac{\partial \phi}{\partial x} = 0; \quad \frac{\partial \varphi}{\partial x} = 0$$

For convenience, let $\psi = 0$ be on FG. Therefore, $\psi = B'$ on AB and $\psi = -W'$ on ED. (B and W are respectively the flow rates of the brine and the wash water losses. B' and W' are these flow rates per unit thickness of the CW).

BD, (Figures 3 and 4) representing a drainage screen, is a vertical line of constant head (ϕ_0) according to assumption 3, for which:

$$\phi = \phi_0; \quad \varphi = -nUy; \quad \frac{\partial \psi}{\partial x} = nU$$

For convenience, $\varphi_0 = -K\phi_0$.

AG is the unknown bottom of the ice bed, with two boundary conditions. It is a line of constant head and uniform flow rate:

$$(a) \quad \frac{d\phi}{dx} = 0$$

$$(b) \quad \frac{d\psi}{dx} = \frac{B}{A} = B'' = \frac{B'}{b}$$

where A is the cross section area of the CW.

EF, the unknown upper boundary has also two conditions: it is a free surface on which a uniform flow of the wash water is seeping. The two conditions of this boundary are:

$$\frac{d\psi}{dx} = -\frac{W}{A} = -W'' = -\frac{W'}{b}$$

and

$$p = p_g - p_c$$

p_g and p_c are, respectively the pressure of the gas above the free surface and the capillary pressure.

The boundaries of FCW are given in Figure 4. The boundary conditions are the same as for DCW except for the horizontal upper scraped surface EF which is fixed and known for FCW and is a line of constant head (ϕ_h), for which

$$\phi = \phi_h; \quad \varphi = K(\phi_h - \phi_0) - nUh; \quad \frac{\partial \psi}{\partial y} = 0$$

THE GENERAL SOLUTION

The flow pattern in our cases (where AG and EF are sufficiently distant from the screens, according to assumption 4), is nearly identical with the flow pattern in the same domain of an approximate case, where the flow region is extended to infinity in both upward and downward directions. In the approximate case as well as in the actual cases, the lines EF and AG are almost horizontal and the flows in their vicinity are practically uniform. The approximate case is easier to solve than the exact cases.

A complete solution of the problem is obtained when the

complex potential, $\omega(z)$, is found. The complex potential is obtained by using the superposition principle. ω is split into three simpler components:

$$\omega = \omega_1 + \omega_2 + \omega_3 = \varphi_1 + \varphi_2 + \varphi_3 + i(\psi_1 + \psi_2 + \psi_3) \quad (10)$$

ω_1 is the complex potential of a symmetrical flow Q_1 from $y = \infty$ and $y = -\infty$ towards the drainage screens. ω_2 is the complex potential representing a flow, Q_2 which flows from $y = -\infty$ with the screen being an equipotential line and constituting a short-circuit. ω_3 is the complex potential of the uniform flow Q_3 of the liquid confined in the ice bed, with respect to the CW due to the movement of the porous bed. The flow rates Q_1 , Q_2 , and Q_3 are given by

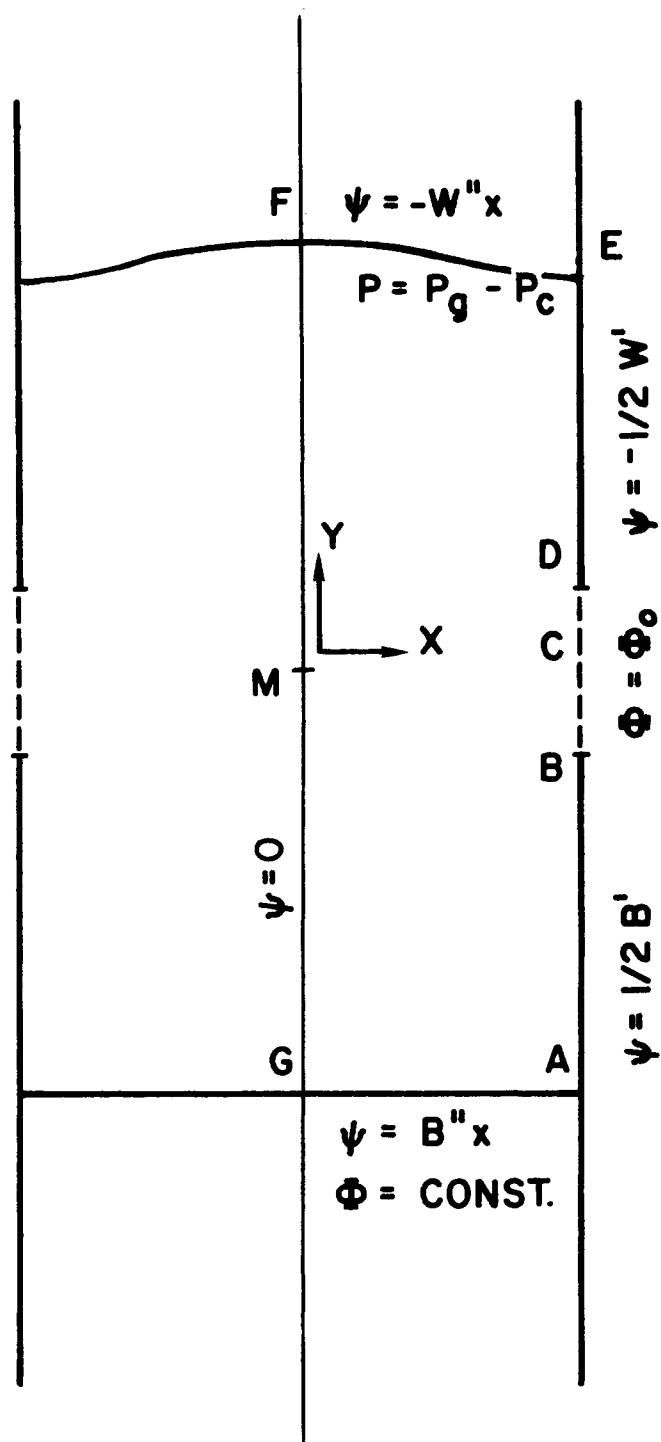


Fig. 3. Boundary conditions in a drained-top counterwasher.

$$Q_1 = \frac{1}{2} (B + W); \quad Q_2 = \frac{1}{2} (B - W) - nUA; \\ Q_3 = nUA \quad (11)$$

The solutions of the three components are obtained by conformal mapping of the complex flow domain from the physical plane to the complex potential plane. The detailed mathematical treatment is given in the appendix A. The final results after Q_1 , Q_2 , and Q_3 , according to Equations (11) are substituted into the equations of appendix A, are:

$$\varphi(x;y) = \frac{B' + W'}{4\pi} \sinh^{-1} M_1^{1/2} \\ - \frac{(B' - W' - 4nUb) y}{4\pi |y|} \sinh^{-1} M_2^{1/2} - nUy \quad (12)$$

$$\psi(x;y) = - \frac{(B' + W')y}{4\pi |y|} \sin^{-1} N_1^{1/2} \\ + \frac{B' - W' - 4nUb}{4\pi} \sin^{-1} N_2^{1/2} + nUx \quad (13)$$

$M_1(x;y)$, $M_2(x;y)$, $N_1(x;y)$ and $N_2(x;y)$ are given in Equations (16A) and (27A) in appendix A.

At the bottom of the ice bed the flow is practically uniform and the potential becomes a linear function of y only:

$$\varphi = -B''y + S(B'; W'; nUb; a/b) \quad (14)$$

Similarly the potential at the vicinity of the upper boundary EF is:

$$\varphi = W''y + T(B'; W'; nUb; a/b) \quad (15)$$

The detailed mathematical development, which yields Equations (14) and (15), is also given in appendix A. The functions S and T are given in Equations (33A) and (34A) in this appendix.

The field of the piezometric head is obtained from the potential, solving Equation (7). Substituting $\varphi_0 = -K\phi_0$ we get

$$\phi(x;y) = \phi_0 + \frac{\varphi(x;y) + nUy}{K} \quad (16)$$

The field of the hydrostatic pressure is obtained from Equations (16) and (2)

$$p(x;y) = \gamma[\phi(x;y) - y] \\ = \gamma \left[\phi_0 + \frac{\varphi(x;y) + (nU - K)y}{K} \right] \quad (17)$$

The fields of the components of the superficial velocity are obtained from the partial derivatives of either φ or ψ according to the defining Equations (5).

$\varphi(x;y)$ in Equations (16), (17), and (5) is taken from Equation (12), (14), or (15).

APPLICATIONS OF THE GENERAL SOLUTION (DCW)

The Elevation of the Water Free Surface

The relationship between the height (h) of the water free surface and the other parameters is obtained from Equation (17). Substituting $y = h$, the boundary condition $p(h) = p_g - p_c$ and $\varphi(x;y)$ from Equation (14) into (17) we get:

$$p_g - p_c = \gamma\phi_0 + \frac{W''h + T + (nU - K)h}{K} \gamma \quad (18)$$

The solution of (18) is:

$$h = \frac{K \left(\phi_0 + \frac{p_c - p_g}{\gamma} \right) + T}{K - (nU + W'')} \quad (19)$$

The Cross Section Area of the DCW

The unsaturated zone in DCW can exist only if

$$nU + W'' < K \quad (20)$$

As U approaches $1/n(K - W'')$, h approaches infinity. Therefore, the cross section area, A , of a column with a given volumetric ice rate capacity, I , has a theoretical limit, A_{\min} :

$$A = \frac{I}{(1-n)U} \geq A_{\min} = \frac{nI}{(1-n)(K - W'')} \quad (21)$$

Considering fluctuations and deviations of I , K , and n from the presumed values, it is recommended that

$$A \geq 1.3 A_{\min} \quad (22)$$

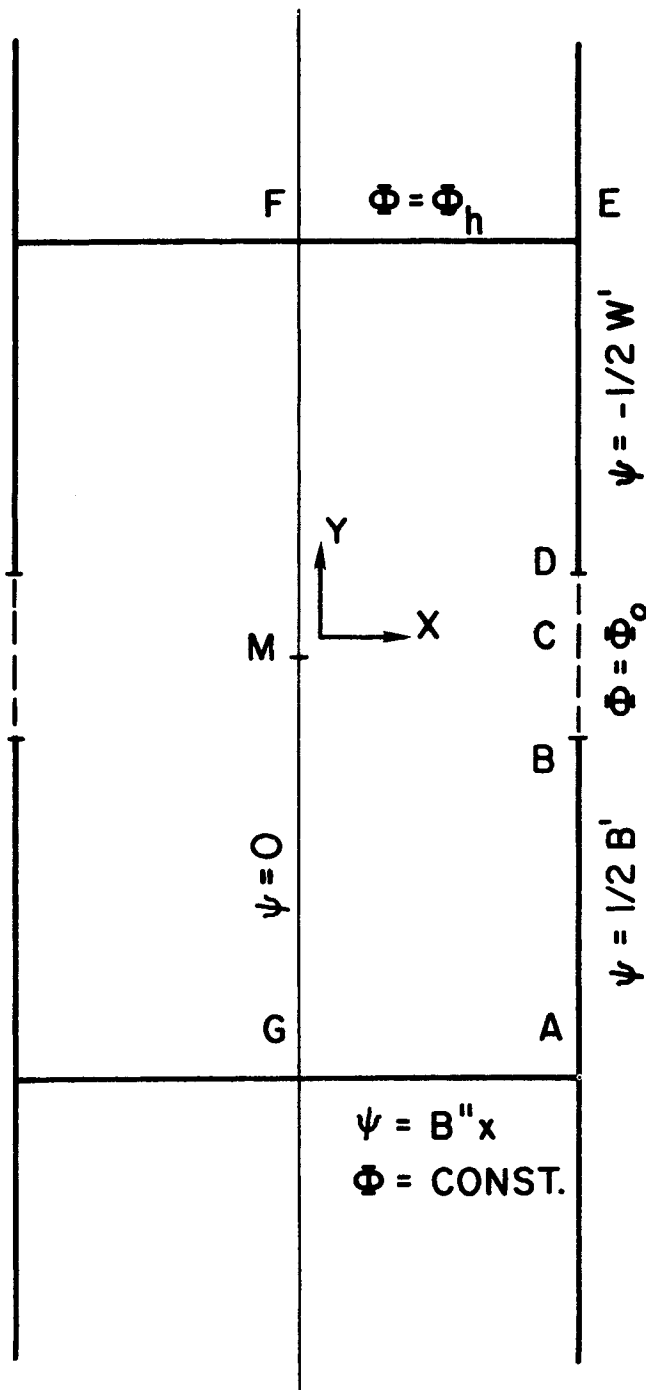


Fig. 4. Boundary conditions in a flooded counterwasher.

The Piezometric Head on the Screens

From Equation (20), the denominator of the right hand side of Equation (19) is positive. Thus the numerator of (19) has to be positive as well. In the vacuum freezing process this condition is always satisfied since ϕ_0 is positive, and $p_g < p_c$ (see appendix B). It is easy to prove that the last term in the numerator of the said expression is also positive. In this process ϕ_0 has to be as small as possible, in order to have a short column. The smallest value of ϕ_0 for which the screens are kept submerged is

$$\phi_0 = a + \frac{p_b}{\gamma} \leq a + 60 \text{ mm.} \quad (23)$$

where p_b is the absolute boiling pressure of the brine.

In the secondary refrigerant freezing process, $p_g \gg p_c$. ϕ_0 has to be high so that the numerator of the right hand side of (19) should be positive and that h should be considerably higher than a . Otherwise, the gas from the upper zone may break and flow through the ice to the screens.

The Depth of the Bottom of the Ice Bed

The unknown depth of the ice bed, d , below the center of the screens is obtained, like h , from Equation (17). In a steady state the sum of the components of the forces acting on the ice bed (including the liquids confined in it) in any direction equals zero. In the vertical direction:

$$\Sigma F_y = Ap(-d) - Ap_g(h) - G - F_r = 0 \quad (24)$$

$p(-d)$ is obtained from Equation (17) into which $\phi(x; y)$ is substituted from Equation (14) with $y = -d$.

$p_g(h)$ is the external pressure on the upper surface of the ice bed: $p_g(h) = p_g$.

G is the total weight of the ice bed

$$G = A(h + d)\gamma + Ah^*\bar{\gamma}^* \quad (25)$$

where

$$\bar{\gamma} = n\gamma + (1 - n)\gamma_i; \bar{\gamma}^* = m\gamma^* + (1 - n)\gamma_i \quad (26)$$

$\bar{\gamma}$ is the average specific weight at the saturated zone. γ^* is the average specific weight at the unsaturated zone, the mean height of which is h^* . γ_i is the specific weight of ice, γ^* and m are respectively the average specific weight and the volume fraction of the liquids in the unsaturated zone.

F_r is the sum of the external forces (friction and resistance of the scrapers) opposing the rising of the ice bed. F_r depends on many factors and cannot be predicted analytically. There are, however, experimental data for F_r . In the Eilat desalination plant (Israel), for instance, $F_r \cong 5 Ab\gamma$.

By substituting Equations (17), (14), and (25) into Equation (24), a linear equation with one unknown, d , is obtained:

$$\phi_0\gamma + \frac{B''d\gamma}{K} - \frac{S\gamma}{K} + \gamma d \left(1 - \frac{nU}{K} \right) = p_g + (h + d)\bar{\gamma} + h^*\bar{\gamma}^* + \frac{F_r}{A} \quad (27)$$

The solution of Equation (27) is:

$$d = \frac{K(h\bar{\gamma} + h^*\bar{\gamma}^* + F_r/A + p_g - \gamma\phi_0) + \gamma S}{\gamma(B'' - nU) + K(\gamma - \bar{\gamma})} \quad (28)$$

APPLICATION OF THE GENERAL SOLUTION FOR THE DESIGN OF FCW

The Height of the Upper (Scraped) Surface

The value of h in FCW is determined by different con-

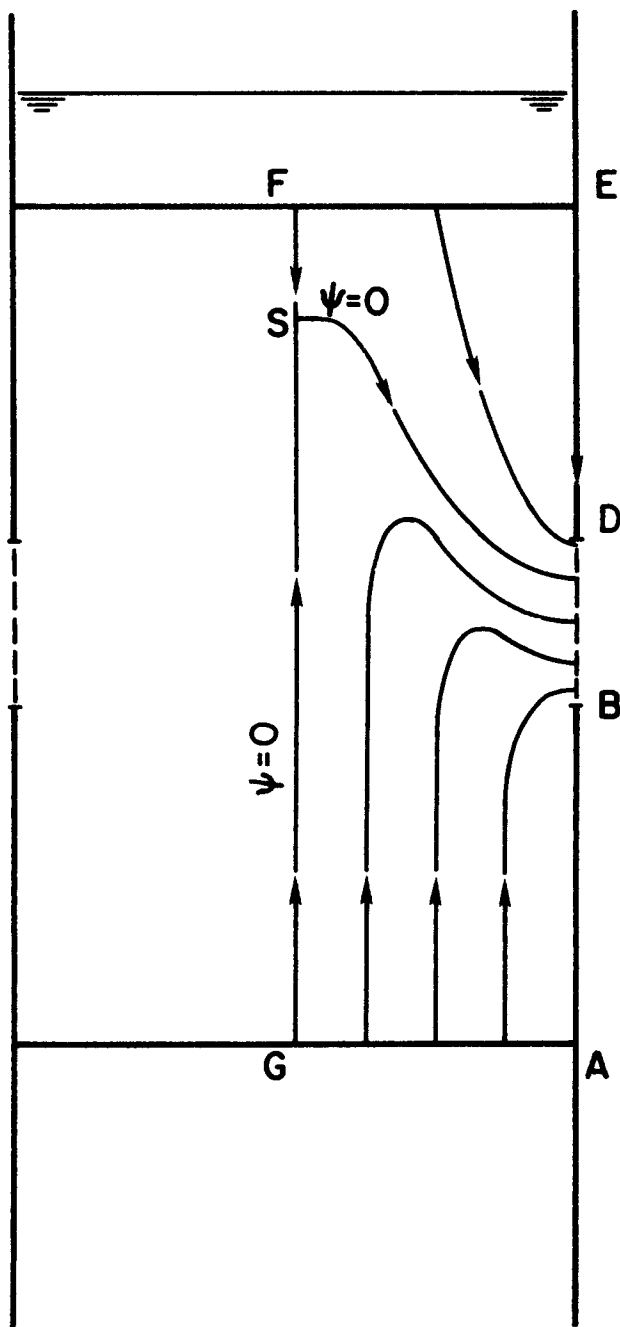


Fig. 5. Schematic streamlines in a flooded counterwasher; normal operation.

siderations than those related to DCW. In both CWs the lower zone of the ice bed is occupied by the brine, and the upper zone is occupied by the wash water. The streamline, which separates these two zones ($\psi = 0$) has a peak on the central vertical line ($x = 0$). This is the stagnation point S (see Figure 5). The height of the stagnation point, y_s , is significant for the design of FCW. Unlike DCWs, in flooded ones there is a danger that part of the brine may flow through the upper boundary (the scraped surface) to the pressurized wash water and contaminate it. The streamlines in such a case are shown in Figure 6. This happens when $h < y_s$. In DCW this cannot happen, because the existence of the unsaturated zone and the uniform downward flow of wash water through it prevents such a situation.

In order to determine h , the value of y_s has to be calcu-

lated first. At the stagnation point $\tilde{q} = 0$ that is,

$$q_x = 0; \quad q_y = 0 \quad (29)$$

The first condition gives, due to the symmetry of the flow pattern, $x_s = 0$.

The second one yields y_s . q_s is obtained by differentiation of φ from Equation (12), according to the defining of Equation (5) with $x = 0$.

The result, after some algebraic manipulation is an equation with one unknown, y_s :

$$q_y(0; y_s) = nU + \frac{(B'' - nU) \exp\left(-\frac{\pi y_s}{b}\right) - (nU + W'')}{\left[1 + 2 \cosh \frac{\pi a}{b} \exp\left(-\frac{\pi y_s}{b}\right) + \exp\left(-\frac{2\pi y_s}{b}\right)\right]^{1/2}} = 0 \quad (30)$$

The solution is, approximately (with less than 1/2 % error for practical plants where $a \leq \frac{1}{2} b$):

$$y_s = \frac{b}{\pi} \ln \frac{B'' + 2 nU \sinh^2 \frac{\pi a}{2b}}{W''} \quad (31)$$

From the economic point of view, it is desirable that the water losses will be small, $W \leq 0.05I$. This amount is sufficient for the removal of the salts. In practical cases $B'' \cong 3.5 I''$; $nU \cong I''$ and $a \cong 0.1 b$. The lower limit of y_s is, therefore:

$$y_{s \min} = \frac{b}{\pi} \ln \frac{3.5 + 2 \sinh^2 \frac{\pi}{20}}{0.05} = 1.35 b$$

The height h of the scraped surface has to be considerably higher than y_s , since in current operation nonsteady states and deviations from the designed state may occur. Thus it is recommended to take

$$h \cong 1.3 y_s \quad (32)$$

Unlike DCW, in FCW h is independent of the hydraulic conductivity of the ice bed.

The Pressure on the Scraped Surface

The pressure p_h under which the wash water should be supplied to the reservoir above the scraped surface in order to ensure the proper flow rate of wash water is obtained from Equation (17), after substituting φ as given by Equation (15) with $y = h$.

$$p_h = \gamma \left[\phi_0 + \frac{T + (nU + W'' - K)h}{K} \right] \quad (33)$$

The Cross Section Area

Unlike DCW, there are no physical limits for the cross section area (or for the rising velocity of the ice bed) in FCW, except the compaction of the ice bed on which too little experimental and theoretical information exists.

The Piezometric Head on the Screens

ϕ_0 should be taken as low as possible as in the case of DCW in the vacuum freezing process [Equation (23)].

The Depth of the Bottom of the Ice Bed

The calculation of d in FCW is essentially the same as for DCW, with p_h from Equation (33) replacing p_g and with $h^* = 0$.

$$d = \frac{K(h\tilde{\gamma} + F_r/A + p_h - \gamma \phi_0) - \gamma S}{\gamma(B'' - nU) + K(\gamma - \tilde{\gamma})} \quad (34)$$

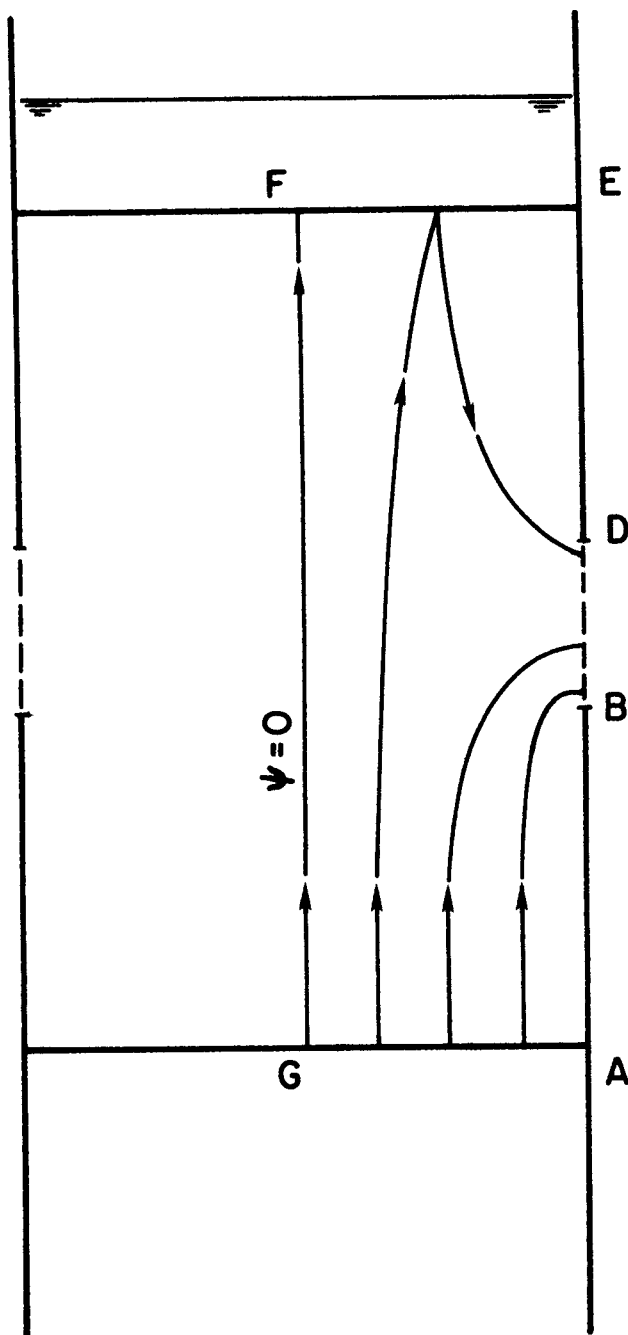


Fig. 6. Schematic streamlines in a flooded counterwasher; malfunctioning.

CONCLUSIONS

In order to design a CW, the dimensions, the brine flow rate, B and the boundary conditions, ϕ_0 and p_h have to be determined from the known or assumed parameters (I and W being the requirements, K , n , F , p_g and p_c being experimental data).

Previously the unknown parameters have been determined according to experimental results. The present analysis, Equations (19) to (28) for DCW and (31) to (34) for FCW, enable the direct calculation of the vertical dimensions of the ice bed (above and below the screens) and of the boundary parameters, leaving only four parameters to be determined experimentally or arbitrarily (b , A , a and B). Furthermore, the mentioned equations, together with economical and engineering data, enable also the in-

direct computation of these four parameters by optimization of the CW, rather than the experimental or arbitrary determination of these parameters. The optimization, however, is beyond the scope of this work due to the large amount of economical and engineering data involved and the length of the optimization process.

ACKNOWLEDGMENT

This work was supported by the Technion, Israel Institute of Technology (CV-225) and by Israel Desalination Engineering (Zarchin Process), Tel Aviv, Israel.

NOTATION

a	= half the height of the drainage screens
A	= cross section area of the CW
b	= half the width of the CW
B	= brine flow rate (volume per unit time)
d	= distance from the bottom of ice bed to the center of the screens
D	= hydraulic mean diameter of the ice particles
F	= external forces acting on ice bed
f, g	= auxiliary geometric functions
G	= weight of ice bed and the liquids in it
g	= gravity acceleration
h	= height of upper boundary
I	= volumetric ice rate capacity (volume per unit time)
k	= permeability of ice bed
K	= hydraulic conductivity of ice bed (length per unit time)
m	= liquid fraction in the unsaturated zone
M, N	= auxiliary geometric functions
n	= porosity of ice bed
p	= hydrostatic pressure
q	= superficial velocity
Q	= flow rate
R	= integration constant
S, T	= kinematic constants of the CW
U	= ice velocity
W	= wash water losses flow rate (volume per unit time)
x, y	= coordinates
z	= complex variable of geometry

Greek Letters

γ	= specific weight (per unit volume)
ζ	= complex auxiliary variable
μ	= viscosity (dynamic)
ρ	= density
σ	= surface tension
φ	= potential of the specific discharge
ϕ	= piezometric head
ψ	= stream function
ω	= complex potential

Subscripts

b	= boiling
c	= capillary
g	= gas
h	= upper boundary
i	= ice
s	= stagnation point
x, y	= horizontal and vertical vector components
0	= drainage screens
$1, 2, 3$	= components of superposition

Superscripts

$\bar{}$	= average
\sim	= vector
$'$	= per unit thickness of CW

"	= per unit cross section area of CW
*	= unsaturated zone

LITERATURE CITED

1. Barduhn, A. J., "The Freezing Process for Water Conversion". 1st International Symposium on Water Desalination SWD/88 (1965).
2. Bosworth, C. M., A. J. Barduhn, S. A. Carfagno, and D. J. Sandell, Office of Saline Water, Res. and Devel. Prog. Rpt. No. 23 (1959).
3. *Ibid.*, Progr. Rpt. No. 32 (1959).
4. Hahn, W. J., *Saline Water Symposium, Freezing and Ion Adsorption* Office of Saline Water (1965).
5. ———, B. S. Burns, R. S. Fullerton, and D. J. Sandell, Office of Saline Water, Res. Devel. Progr. Rpt. No. 113 (1964).
6. Kuivenhoven, A. C. J., "Wash Columns for Removal of Ice from Aqueous Solutions", Delft Symposium (1966).
7. Mixon, F. O., Contract 379, Office Saline Water (1964).
8. Sherwood, T. K. and Brian, P. L. T., Office Saline Water Res. Devel. Progr. Rpt. No. 179 (1965).
9. Wiegandt, H. F., "Saline Water Conversion," *Am. Chem. Soc.*, No. 27, Washington (1960).
10. Dagan, G., and A. Barak, "Flow Pattern in the Saturated Zone of Ice Counterwashers" (In Hebrew), Technion, Israel Inst. Tech., Haifa (1967).
11. Schwartz, J., and R. F. Probstein, Mass. Inst. Tech. Publ. No. 67-7, (1967).
12. Wiegandt, H. F., R. L. Von Berg, and J. P. Leinroth, Office Saline Water Grant No. 14-01-0001-1141, Cornell Univ., Ithaca, N. Y. (1967).
13. Florin, V. A., "Teoria uplotrenia Zemlianih," Moscow (1948).
14. Scheidegger, A. E., "The Physics of Flow Through Porous Media," University of Toronto Press, Canada (1960).

Manuscript received January 13, 1968; revision received June 14, 1968; paper accepted June 17, 1968.

APPENDIX A

The Solution at the First Component

The first component is solved by Schwarz-Christophel conformal mapping. Because of the symmetry it is sufficient and easier to solve the flow equations for one quarter, say the lower right one, of the flow domain. The latter is first mapped from the physical plane (Fig. 1A) to the upper part of the auxiliary plane ζ (Fig. 2A) and the boundaries are mapped on the real axis so that

$$\zeta_A = -\infty; \quad \zeta_C = -1; \quad \zeta_M = 1 \quad (1A)$$

The mapping is achieved by

$$\frac{dz}{d\zeta} = R' (\zeta - \zeta_C)^{-1/2} (\zeta - \zeta_M)^{-1/2} = \frac{R'}{(\zeta^2 - 1)^{1/2}} \quad (2A)$$

Integrating, we get

$$z = R' \cosh^{-1} \zeta + R'' \quad (3A)$$

The constants R' and R'' are obtained by substituting the complex values of the points C and M in the z and ζ planes into Equation (3A). The solution is:

$$R' = -i \frac{b}{\pi}; \quad R'' = 0 \quad (4A)$$

Thus

$$z = -i \frac{b}{\pi} \cosh^{-1} \zeta; \quad \zeta = \cosh \frac{\pi iz}{b} \quad (5A)$$

Substituting the complex value of the point B into Equation (5A) we get

$$\zeta_B = \cosh \frac{\pi i(b - ia)}{b} = -\cosh \frac{\pi a}{b} \quad (6A)$$

The flow domain is mapped from the complex potential (ω) plane (Fig. 3A) to the auxiliary plane ζ in a similar way.

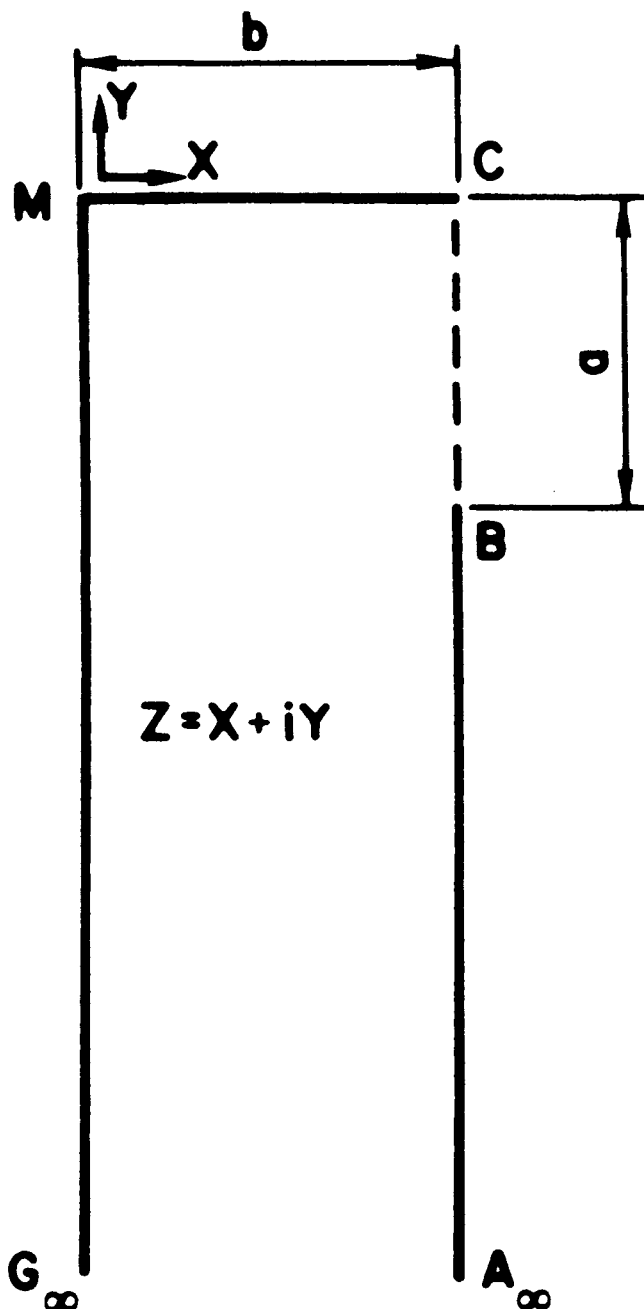


Fig. 1A. The $\frac{1}{4}$ flow domain in the physical plane.

$$\frac{d\omega_1}{d\zeta} = R_1' (\zeta - \zeta_B)^{-1/2} (\zeta - \zeta_C)^{-1/2} \quad (7A)$$

Integrating and substituting ζ_C and ζ_B from (1A) and (6A) we get:

$$\omega_1 = R_1' \cosh^{-1} \frac{2\zeta + \cosh \frac{\pi a}{b} + 1}{\cosh \frac{\pi a}{b} - 1} + R_1'' \quad (8A)$$

The constants R_1' and R_1'' are obtained by substituting the complex values of the points C and B in the ζ and ω planes into Equation (8A). The solution is:

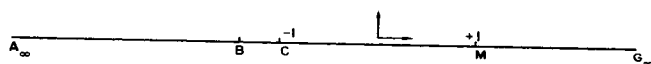


Fig. 2A. The $\frac{1}{4}$ flow domain in the auxiliary plane.

$$R_1' = \frac{Q_1'}{2\pi}; \quad R_1'' = 0 \quad (9A)$$

Thus:

$$\begin{aligned} \omega_1 &= \frac{Q_1'}{2\pi} \cosh^{-1} \frac{2\zeta + \cosh \frac{\pi a}{b} + 1}{\cosh \frac{\pi a}{b} - 1} \\ &= \frac{Q_1'}{2\pi} \cosh^{-1} \frac{\cos \frac{\pi z}{b} + \cosh^2 \frac{\pi a}{2b}}{\sinh^2 \frac{\pi a}{2b}} \end{aligned} \quad (10A)$$

or

$$\cosh \frac{2\pi\omega_1}{Q_1'} = \frac{\cos \frac{\pi z}{b} + \cosh^2 \frac{\pi a}{2b}}{\sinh^2 \frac{\pi a}{2b}} \quad (11A)$$

The equality of the real and imaginary parts of (11A) yields two real equations:

$$\begin{aligned} \cosh \frac{2\pi\varphi_1}{Q_1'} \cos \frac{2\pi\psi_1}{Q_1'} &= \frac{\cosh \frac{\pi y}{b} \cos \frac{\pi x}{b} + \cosh^2 \frac{\pi a}{2b}}{\sinh^2 \frac{\pi a}{2b}} = f_1(x, y) \end{aligned} \quad (12A)$$

$$\sinh \frac{2\pi\varphi_1}{Q_1'} \sin \frac{2\pi\psi_1}{Q_1'} = - \frac{\sinh \frac{\pi y}{b} \sin \frac{\pi x}{b}}{\sinh^2 \frac{\pi a}{2b}} = g_1(x, y) \quad (13A)$$

$\varphi_1(x, y)$ and $\psi_1(x, y)$ are derived from (12A) and (13A) after some algebraic manipulations:

$$\varphi_1(x, y) = \frac{Q_1'}{2\pi} \sinh^{-1} M_1^{1/2} \quad (14A)$$

$$\psi_1(x, y) = - \frac{Q_1' y}{2\pi |y|} \sin^{-1} N_1^{1/2} \quad (15A)$$

where:

$$\begin{aligned} M_1(x, y) &= \frac{1}{2} [(f_1^2 + g_1^2 - 1)^2 + 4g_1^2]^{1/2} \\ &\quad + \frac{1}{2} (f_1^2 + g_1^2 - 1) \end{aligned} \quad (16A)$$

$$\begin{aligned} N_1(x, y) &= \frac{1}{2} [(f_1^2 + g_1^2 - 1)^2 + 4g_1^2]^{1/2} \\ &\quad - \frac{1}{2} (f_1^2 + g_1^2 - 1) \end{aligned}$$

Far from the screens, $-y \geq a + b$, the value of the potential φ_1 is high and the flow is practically uniform:

$$\begin{aligned} -\sinh \frac{\pi y}{b} &\cong \frac{1}{2} \exp \left(-\frac{\pi y}{b} \right); \\ \sinh \frac{2\pi\varphi_1}{Q_1'} &\cong \frac{1}{2} \exp \left(\frac{2\pi\varphi_1}{Q_1'} \right); \quad \psi \cong \frac{Q_1' x}{2b} \end{aligned} \quad (17A)$$

Substituting (17A) into (15A) we get:

$$\exp \left(\frac{2\pi\varphi_1}{Q_1'} \right) = \frac{\exp \left(-\frac{\pi y}{b} \right)}{\sinh^2 \frac{\pi a}{2b}} \quad (18A)$$

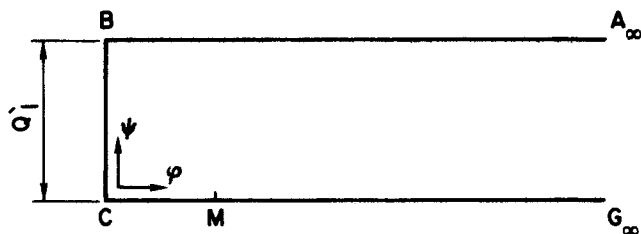


Fig. 3A. The $\frac{1}{4}$ flow domain in the complex potential plane ω : component 1.

$$\varphi_1 = -\frac{Q_1'y}{2b} - \frac{Q_1'}{\pi} \ln \sinh \frac{\pi a}{2b} \quad (19A)$$

At the upper part of the CW ($y > a + b$) due to the symmetry

$$\varphi_1 = \frac{Q_1'y}{2b} - \frac{Q_1'}{\pi} \ln \sinh \frac{\pi a}{2b} \quad (20A)$$

The Second Component

The solution of the second component is similar to that of the first one. The flow domain in the complex potential plane (Fig. 4A) is mapped to the auxiliary plane by

$$\frac{d\omega_2}{d\xi} = R_2' (\xi - \xi_B)^{-1/2} (\xi - \xi_M)^{-1/2} \quad (21A)$$

The derivation is the same as in Equations (7A) to (10A) with $\xi_M (=1)$ replacing $\xi_C (= -1)$ and Q_2' replacing Q_1' :

$$\begin{aligned} \omega_2 &= \frac{Q_2'}{2\pi} \cosh^{-1} \frac{2\xi + \cosh \frac{\pi a}{b} - 1}{\cosh \frac{\pi a}{b} + 1} \\ &= \frac{Q_2'}{2\pi} \cosh^{-1} \frac{\cos \frac{\pi z}{b} + \sinh^2 \frac{\pi a}{2b}}{\cosh^2 \frac{\pi a}{2b}} \end{aligned} \quad (22A)$$

Equation (22A) is similar to Equation (10A) with ω_2 and Q_2' replacing ω_1 and Q_1' , $\sinh \frac{\pi a}{2b}$ replacing $\cosh \frac{\pi a}{2b}$ and vice versa. The following equations are similar to Equations (11A) to (20A) in the same way. Thus:

$$\begin{aligned} \cosh \frac{2\pi\varphi_2}{Q_2'} \cos \frac{2\pi\psi_2}{Q_2'} &= \frac{\cosh \frac{\pi y}{b} \cos \frac{\pi x}{b} + \sinh^2 \frac{\pi a}{2b}}{\cosh^2 \frac{\pi a}{2b}} = f_2(x; y) \quad (23A) \end{aligned}$$

$$\sinh \frac{2\pi\varphi_2}{Q_2'} \sin \frac{2\pi\psi_2}{Q_2'} = -\frac{\sinh \frac{\pi y}{b} \sin \frac{\pi x}{b}}{\cosh^2 \frac{\pi a}{2b}} = g_2(x; y) \quad (24A)$$

$$\varphi_2(x; y) = -\frac{Q_2'y}{2\pi|y|} \sinh^{-1} M_2^{1/2} \quad (25A)$$

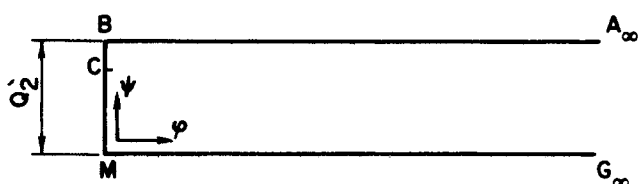


Fig. 4A. The $\frac{1}{4}$ flow domain in the complex potential plane ω : component 2.

$$\psi_2(x; y) = \frac{Q_2'}{2\pi} \sin^{-1} N_2^{1/2} \quad (26A)$$

$$\begin{aligned} M_2(x; y) &= \frac{1}{2} [(f_2^2 + g_2^2 - 1)^2 + 4g_2^2]^{1/2} \\ &\quad + \frac{1}{2} (f_2^2 + g_2^2 - 1) \end{aligned} \quad (27A)$$

$$\begin{aligned} N_2(x; y) &= \frac{1}{2} [(f_2^2 + g_2^2 - 1)^2 + 4g_2^2]^{1/2} \\ &\quad - \frac{1}{2} (f_2^2 + g_2^2 - 1) \end{aligned}$$

For $-y \geq a + b$

$$\varphi_2 \cong -y \frac{Q_2'}{2b} - \frac{Q_2'}{\pi} \ln \cosh \frac{\pi a}{2b} \quad (28A)$$

and for $y \geq a + b$, due to the nonsymmetry of this component

$$\varphi_2 \cong -y \frac{Q_2'}{2b} + \frac{Q_2'}{\pi} \ln \cosh \frac{\pi a}{2b} \quad (29A)$$

The Third Component

The solution of this component is direct, since the flow is uniform:

$$\omega_3 = i Q_3' z = i n U z \quad (30A)$$

$$\varphi_3 = -n U y \quad (31A)$$

$$\psi_3 = n U x \quad (32A)$$

The Combined Solution

The general solution of the approximate case is obtained by summing up the solutions of the components:

$$\varphi = \varphi_1 + \varphi_2 + \varphi_3; \quad \psi = \psi_1 + \psi_2 + \psi_3$$

For large value of $|y|$, φ_1 and φ_2 are taken from Equations (19A) and (28A) or (20A) and (29A), and the results of the summation in both cases converge after substituting Q_1 , Q_2 , and Q_3 according to Equation (11) to the following expressions:

for $-y \geq a + b$

$$\begin{aligned} S = \varphi(x; y) + B'y &= -\frac{1}{2\pi} \left[(B' + W') \ln \frac{1}{2} \sinh \frac{\pi a}{b} \right. \\ &\quad \left. - 2(W' + 2nUb) \ln \cosh \frac{\pi a}{2b} \right] \end{aligned} \quad (33A)$$

and for $y \geq a + b$

$$\begin{aligned} T = \varphi(x; y) - W''y &= \frac{1}{2\pi} \left[(B' + W') \ln \coth \frac{\pi a}{2b} \right. \\ &\quad \left. - 2(W' + 2nUb) \ln \cosh \frac{\pi a}{2b} \right] \end{aligned} \quad (34A)$$

APPENDIX B

The capillary pressure in a well wetted porous medium is, according to Scheidegger (14)

$$p_c = \frac{6(1-n)\sigma}{nD}$$

In typical washers, $n \cong 0.5$. For cold water the surface tension $\sigma = 7.3 \times 10^{-3}$ kg./m. The minimum p_c is attained when D , the hydraulic mean diameter of the ice particles, is maximal, that is $D = 0.5$ mm. $= 0.5 \times 10^{-3}$ m. (assumption b.)

$$p_c \text{ min.} = \frac{6 \times 0.5 \times 7.3 \times 10^{-3}}{0.5 \times 0.5 \times 10^{-3}} = 87.6 \text{ kg./sq.m.}$$

In the vacuum freezing process, $p_g \cong 5$ mm. Hg $= 68$ kg./sq.m., therefore, $p_g < p_c$.